AGU PUBLICATIONS

JGR

Journal of Geophysical Research: Space Physics

RESEARCH ARTICLE
10.1002/2016JA023088

**Key Points:**
- CADI ionosonde Doppler drifts are validated over the equator
- Seasonal variations of PRE drifts have been investigated
- Compare the Doppler vertical drifts with drifts as obtained by using virtual height and model

**Correspondence to:**
S. Sripathi,
ssripathi.iig@gmail.com

**Citation:**
Sripathi, S., R. Singh, S. Banola, S. Sreekumar, K. Emperumal, and C. Selvaraj (2016), Characteristics of the equatorial plasma drifts as obtained by using Canadian Doppler ionosonde over southern tip of India, *J. Geophys. Res. Space Physics*, *121*, doi:10.1002/2016JA023088.

Received 20 JUN 2016
Accepted 31 JUL 2016
Accepted article online 6 AUG 2016



# Characteristics of the equatorial plasma drifts as obtained by using Canadian Doppler ionosonde over southern tip of India

**S. Sripathi[1,2], Ram Singh[1], S. Banola[1], Sreeba Sreekumar[1], K. Emperumal[3], and C. Selvaraj[3]**

[1]Indian Institute of Geomagnetism, Mumbai, India, [2]On deputation to ICTP, Trieste, Italy, [3]Equatorial Geophysical Research Laboratory, Indian Institute of Geomagnetism, Tirunelveli, India

**Abstract** We present here characteristics of the Doppler drift measurements over Tirunelveli (8.73°N, 77.70°E; dip 0.5°N), an equatorial site over Southern India using Doppler interferometry technique of Canadian ionosonde. Three-dimensional bulk motions of the scatterers as reflected from the ionosphere are derived by using Doppler interferometry technique at selected frequencies using spaced receivers arranged in magnetic E-W and N-S directions. After having compared with Lowell's digisonde drifts at Trivandrum, we studied the temporal and seasonal variabilities of quiet time drifts for the year 2012. The observations showed higher vertical drifts during post sunset in the equinox followed by winter and summer seasons. The comparison of Doppler vertical drifts with the drifts obtained from (a) virtual height and (b) Fejer drift model suggests that Doppler vertical drifts are relatively higher as compared to the drifts obtained from model and virtual height methods. Further, it is seen that vertical drifts exhibited equinoctial asymmetry in prereversal enhancement quite similar to such asymmetry observed in the spread *F* in the ionograms and GPS L band scintillations. The zonal drifts, on the other hand, showed westward during daytime with mean drifts of ~150–200 m/s and correlated well with equatorial electrojet strength indicating the role of *E* region dynamo during daytime, while they are eastward during nighttime with mean drifts of ~100 m/s resembling *F* region dynamo process. Also, zonal drifts showed large westward prior to the spread *F* onset during autumn equinox than vernal equinox, suggesting strong zonal shears which might cause equinoctial asymmetry in spread *F*.

## 1. Introduction

Electric fields in the equatorial ionosphere are very important for the day-to-day variabilities in the large-scale electrodynamical processes such as equatorial electrojet (EEJ), equatorial ionization anomaly, and equatorial spread *F* (ESF). Hence, measurement of electric fields of the equatorial ionosphere has been made for several decades using both ground- and space-based instruments [*Fejer and Kelley*, 1980; *Kelley*, 1989; *Namboothiri et al*., 1989]. These electric fields are used to understand the plasma density irregularities or density gradients in the ionosphere. The temporal variations in the electron density, density gradients, electric fields, and plasma drift motion as obtained by using these ground- and space-based instruments have provided valuable information about the variable ionosphere. However, routine measurements of these electric fields are at very few locations. Some notable instruments such as Jicamarca incoherent scatter radar and Jicamarca Unattended Long-term Ionosphere and Atmosphere radar are often used to obtain equatorial zonal electric fields [e.g., *Fejer et al*., 1991; *Kudeki and Fawcett*, 1993; *Hysell and Burcham*, 1998]. HF Doppler radars have also been used widely over Indian region to study the density irregularities and the drift motion of the ionosphere [e.g., *Viswanathan et al*., 1992; *Balan et al*, 1992; *Subbarao and Krishnamurthy*, 1994; *Sastri et al*., 1995; *Prabhakaran Nayar and Sreehar*, 2004; *Reddi et al*., 2009]. These observations have proved that ionospheric drifts or electric fields are crucial to understand the electrodynamics of the ionospheric plasma irregularities and related variabilities in the ionosphere. However, it is very difficult to obtain continuously these electric fields or drifts and its variations with solar and geomagnetic activities at all locations. Using satellites such as AE-E, ROCSAT-1, DMSP, and C/NOFS, the temporal and spatial variations of the drifts have been studied extensively [*Fejer et al*., 1995; *Su et al*., 2001; *Burke et al*., 2004; *de La Beaujardière, et al*., 2004]. Using assimilation of the ground- and space-based drift measurements, empirical drift models have been developed [*Scherliess and Fejer*, 1999]. However, since satellites are nonstationary, they cannot provide continuous drift information at all locations at all times, which are essential to understand the day-to-day

variability of the dynamics of the low-latitude ionosphere. The day-to-day variabilities in the ionospheric plasma irregularities or scintillations are very important for space weather point of view. In this respect, one of the simplest and best ground-based instrument that provides vital information about background layering movements over a given location is an ionosonde [*Breit and Tuve*, 1925; *Devies*, 1989; *Reinisch*, 1996]. In the recent past, modern ionosondes have come up with the capability of Doppler interferometry technique through which ionosondes can be used as a radar to detect drift motion of the bulk ionization layers by using fixed frequency operations [*Reinisch*, 1996; *Kouba and Knížová*, 2012; *Bianchi and Altadill*, 2005; *Woodman et al*., 2006]. Ionosondes like Digisonde Portable Sounder (DPS) and Canadian Advanced Digital Ionosonde (CADI) systems are used widely to investigate the drifts for scientific studies as well as for routine monitoring at wide locations [*Bibl and Reinisch*, 1978; *Reinisch*, 1996; *Reinisch et al*., 1998; *Grant et al*., 1995; *Abdu et al*., 1998]. Several investigations are being made by using both zonal and vertical drifts obtained from such ionosonde systems over Brazilian sector [*Abdu et al*., 2003a, 2003b; *Reinisch et al*., 2004]. Over Indian region, HF Doppler radar is being widely used to study the height variation of these drifts [e.g., *Sastri et al*., 1995; *Prabhakaran Nayar and Sreehari*, 2014]. The plasma vortex in the *F* region ionosphere during dusk sector, which is believed to be responsible for the generation of spread *F* onset, has been investigated using vertical and zonal drift motions of the HF Doppler radar over Trivandrum [*Sreehari et al*., 2006; *Mathew and Nayar*, 2012]. Hence, the drift measurements of both horizontal and vertical motions are very important for understanding the day-to-day variability of the ESF irregularities.

The Indian Institute of Geomagnetism (IIG), Mumbai, India, has set up two CADI ionosondes out of which one is set up at one of its regional centers at Tirunelveli, which is an equatorial station and the other at regional center at Allahabad during the year of 2006. Since then, we have been monitoring movement of various ionospheric layers and its dynamics by using these ionosondes. Already, some investigations have been made by using these systems and results have appeared in referred journals [*Nayak et al*., 2014; *Narayanan et al*., 2014; *Tiwari et al*., 2012; *Joshi and Sripathi*, 2016]. However, we have not investigated the drifts using CADI system using larger data. Recently, we made some attempt to investigate the drifts and its dynamics over Tirunelveli during daytime and its correction for its utility [*Joshi and Sripathi*, 2016]. In this paper, we present variability of both vertical and zonal drifts during different seasons and their comparison with available drift model such as *Scherliess and Fejer* [1999]. We also compared zonal drifts with EEJ strength and spread *F*. We also made a comparison with Lowell's digisonde vertical drifts over Trivandrum, which is ~100 km (radial) far. It may be mentioned that the Doppler technique relies mainly on the reflection of the plasma waves from the density inhomogeneities caused due to the plasma instabilities. Due to these density inhomogeneities, the reflected signals received by the four receiver channels from various scattering centers in the sky will yield valuable information about ionospheric movements.

## 2. CADI System Description

The Canadian Advanced Digital Ionosonde (CADI) is a modern digital ionosonde developed for both routine monitoring and scientific research by Scientific Instrumentation Lab, Canada [*MacDougall et al*., 1995; *MacDougall et al*., 1998; *Grant et al*., 1995; *Hussey et al*., 2004]. CADI ionosonde system at Tirunelveli was set up during middle of 2006. Its frequency range is from 1 to 20 MHz. It can be operated under low-resolution (~100 frequencies), medium-resolution (~200 frequencies), and high-resolution (~400 frequencies) operations. The step size of the sweep could be either linear or logarithmic as per user choice. CADI is operated as vertical incidence sounder providing information on the local ionosphere. CADI provides direct information on (a) the echo delay (virtual height) as a function of frequency, (b) the amplitude and phase of the reflected signal, and (c) the Doppler shift due to motion of the reflector at selected frequencies. A complete ionogram requires from a few seconds (at low-frequency resolutions) to several minutes (at high-frequency resolutions). The system integrates phase coding techniques along with solid state electronics to make CADI a powerful tool to probe ionosphere. It has provision to operate between conventional ionogram and drift modes of operations alternately. While the conventional ionogram takes about 10 min to complete one ionogram as per the user selection, between two successive ionograms, the system supports to operate on several independent frequencies as defined by the specifications provided by the user. This sequence can be programmed to continue for every day to get both conventional ionograms as well as drift measurements. Delta-type transmitting antenna with four co-located receivers arranged in magnetic north-south (N-S) and east-west (E-W) directions is used to receive the returned echo. The transmitter uses pulse compression technique by using 13-bit Barker code to increase the signal strength. The peak transmitter power of the system is 600 W. Amplifier units are all solid state

devices. CADI can probe from 90 km to height of 512 km (1020 km) with either 3 or 6 km resolutions. The transmitter and receivers are synchronized to a reference oscillator at 50 MHz by using a direct digital synthesizer unit. To provide more accurate drifts, the phase difference between each antenna pair and phase responses of the receivers is matched and antenna cables are maintained at identical lengths.

The receiver antennas are set up at four mutually spaced, orthogonal locations with the separation between each receiver location is 30 m as per the procedure given by *Wright and Pitteway* [1979]. These four antennas are arranged in magnetic north-south and east-west direction over the equator. Each dipole is an untuned dipole of overall length of 19 m. The center of each dipole is fed to a balanced high input impedance preamplifier. Experimentally, it is shown that phase measurements at four spaced receiving antennas in a square array contain contributions identified with echo polarization and arrival angle [e.g., *Wright and Pitteway*, 1979]. This is based on two properties of the received signal, namely, complimentary polarizations and apparent location of the reflecting surface from where the echo reflected back from the ionosphere.

The equatorial ionosphere is highly dynamic owing to the fact that unique geometry (due to Earth's magnetic field lines are being horizontal at the equator (magnetic)) is responsible for the generation of small-scale density irregularities in the post sunset hours and provides a corrugating surface for reflection/scattering. As a result, the received signal associated with each propagation mode may arrive at the receiver over wide directions. The drift velocity of the medium is related to the Doppler shift as per the *Cannon et al.* [1991].

### 2.1. Typical Equatorial Ionograms and the Satellite Traces as Seen at Tirunelveli

First, we present a typical equatorial ionogram as obtained from Tirunelveli in Figure 1a on 17 March 2015 at 12:30 Indian Standard Time (IST). The ionogram presents a typical variation of frequency with respect to altitude. From the figure, it can be noticed the splitting of *F* layer into $F_1$, $F_2$, and $F_3$ layers during the day which are believed to be due to the combination of (a) production, (b) transport, (c) electrodynamics, and (d) loss processes. In the Figure 1b, we present typical ionogram which is obtained on 18 January 2015 at 20:00 IST to show satellite traces in the ionogram. These satellite traces are believed to be due to modulations in the *F* layer typically by gravity waves just prior to the onset of ESF irregularities in the ionograms [*Tsunoda*, 2008, 2009]. In addition, there are second hop traces which could be due to multiple reflections from the ground and ionosphere [e.g., *Bhaneja et al*., 2009]. In the recent past, several investigations have been made by using satellite traces over equatorial sites during ESF or non-ESF nights and their relation to occurrence of plasma density irregularities including Tirunelveli station [e.g., *Narayanan et al*., 1992]. As observations belong to the March period which is the season for strong spread *F* over India, we may be seeing several satellite traces in the ionogram prior to spread *F*. Figure 1c shows the ionogram on a typical spread *F* night. These are diffused echoes coming from small-scale irregularities in the ionosphere.

### 2.2. Skymaps

Skymaps are used to describe angular position of the scatterers in the sky. Here the overhead point is marked by the plus sign. The color information represents drift velocity. A skymap displays various reflection sources which have been reflected from the ionosphere. This skymap displays the spatial distribution and the Doppler shifts of ionospheric echo sources. A representative skymap at 4 MHz sounding frequency during January 2015 is shown in Figure 2.

### 2.3. North-South and East-West Distance Plots

Figures 3a and 3b show the north-south and east-west distance plot at 400 km distance from the ionosonde station obtained by using 6 MHz frequency. Using this plot, it is possible to see the movement of ionospheric structures. Figure 3a shows the east-west location of received echoes, while Figure 3b shows the north-south location. It is also possible to calculate the distance plot for 200, 100 km. In this example, the sloping features in the north-south panel show that there were ionospheric patches moving northward. The zonal distance plot suggests that they are moving eastward, which is usually the case during nighttimes.

### 2.4. Doppler Drift Measurements

The CADI ionosonde at Tirunelveli was operated alternately between the ionogram mode and drift mode. The CADI was operated in ionogram mode at every 10 min interval interleaved by drift mode of operations at seven independent (fixed) frequencies as per the predefined specifications. We present here drift measurements made at few fixed transmitter frequencies, namely, at 4 MHz, 5 MHz, and 6 MHz that correspond to

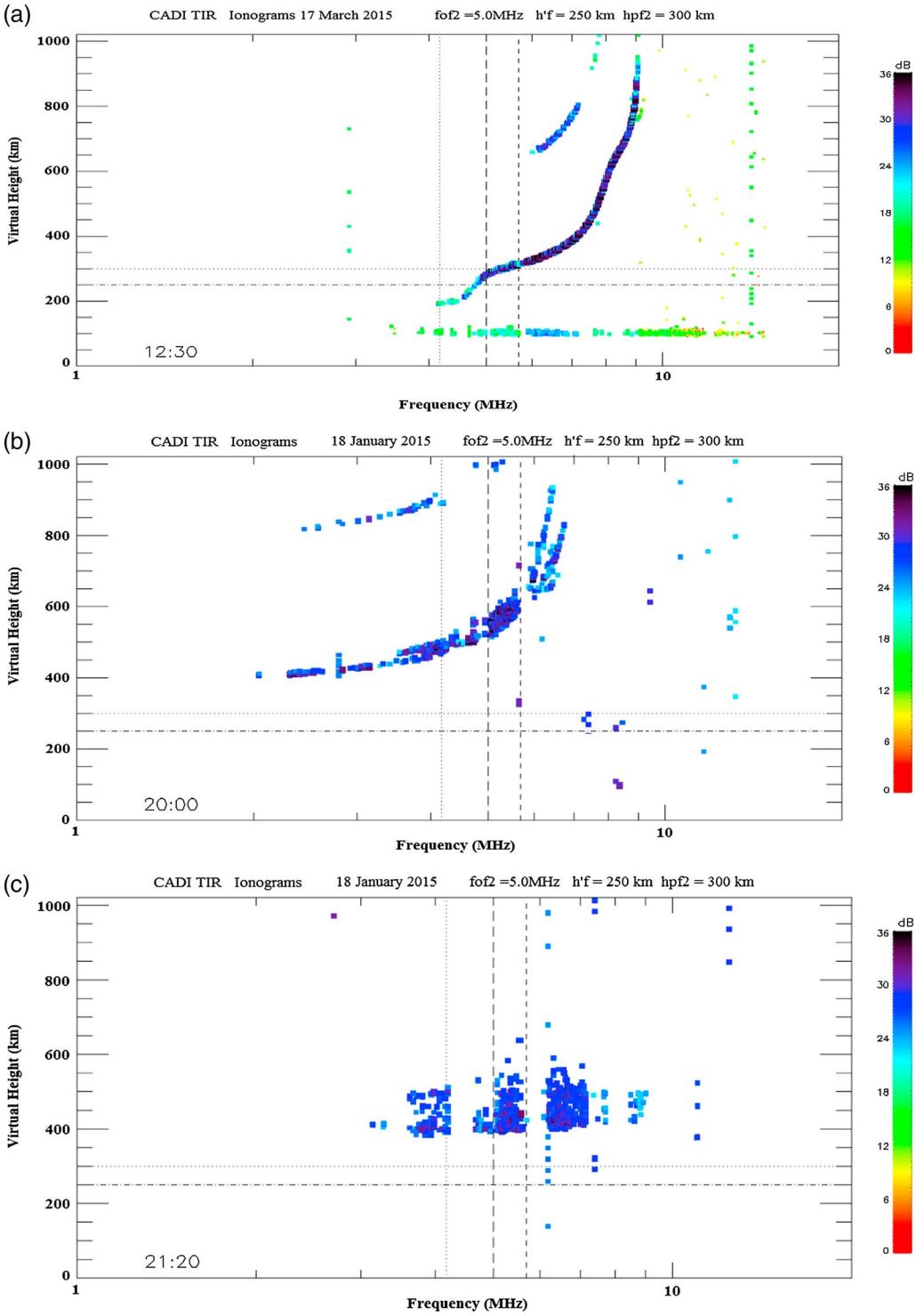


**Figure 1.** The typical ionograms of Tirunelveli during (a) daytime, (b) evening hours, and (c) spread *F* night.

wavelengths ($\lambda$) in the range of 50 m to 75 m. The reflected echoes in terms of I and Q channels for each transmitted frequency using each of the four receivers are further analyzed by using 64-point FFT (fast Fourier transform) complex time series for each antenna. This system was run under 20 pps for drift measurements which means interpulse period of 50 ms. For drift analysis, we used 64-point FFT, which means that the total time length is ~3–4 s. In order to obtain the strongest echo, we applied noise threshold where if the power in

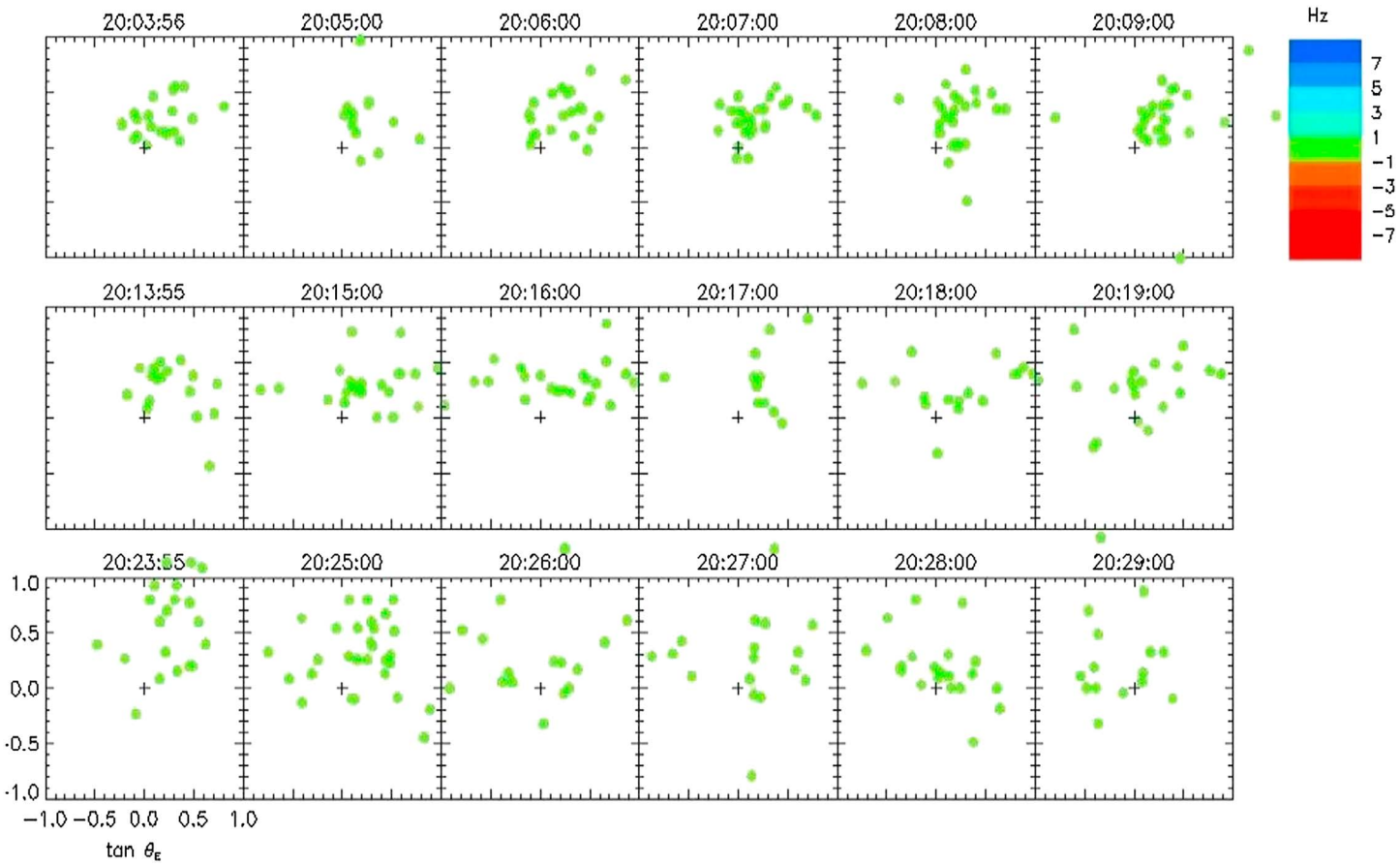


**Figure 2.** The typical skymap over Tirunelveli at different times on 18 January 2015.

each of the Doppler bin of the first antenna is above noise threshold, then that bin is saved for all four antennas. Now Doppler bin data consist of only the strongest part of the Doppler spectrum and are assumed to correspond to an ionospheric reflection point or "source point."

Using cross spectra of the Doppler bin for each north-south (N-S) or east-west (E-W) antenna pair, the Doppler drifts are obtained. While cross phases of the two antenna pairs give the angle of arrival information of the source, variation in the Doppler shift across the skymap shows the bulk motion of the sources. The following assumptions are being made while determining the drift velocities, namely, (a) ionosphere is in steady state and has uniform motion and (b) the motion is mainly horizontal and (c) the source points should have incidence angle that is close to vertical. Since it is assumed that the ionosphere is moving with a uniform bulk motion, the drift velocity being detected by this Doppler interferometer is measure of bulk plasma motion in the ionosphere. Accordingly, the software automatically selects the source points with a maximum angle of arrival of 45°. From Figure 2, this corresponds to maximum tanθN and tanθE values of ±1 that is of primary source to derive the plasma drifts being investigated in this paper. From the spectral phases across the receiving antennas, the source wave vector $k_s$ is determined. The intersection of these $k_s$ vectors with horizontal plane at each frequency generates skymaps of the source locations.

The drift velocity of the medium can be related to the Doppler shift as per the *Cannon et al.* [1991] by using the following equation:

$$d_s = \frac{1}{\pi} v.k_s \text{where } s = \text{source index},$$

$D_s$ = Doppler shift of reflection point at the receiving antennas
$v$ = source velocity
$k_s$ = unit vector from the ionospheric reflection point, $s$ toward receiver

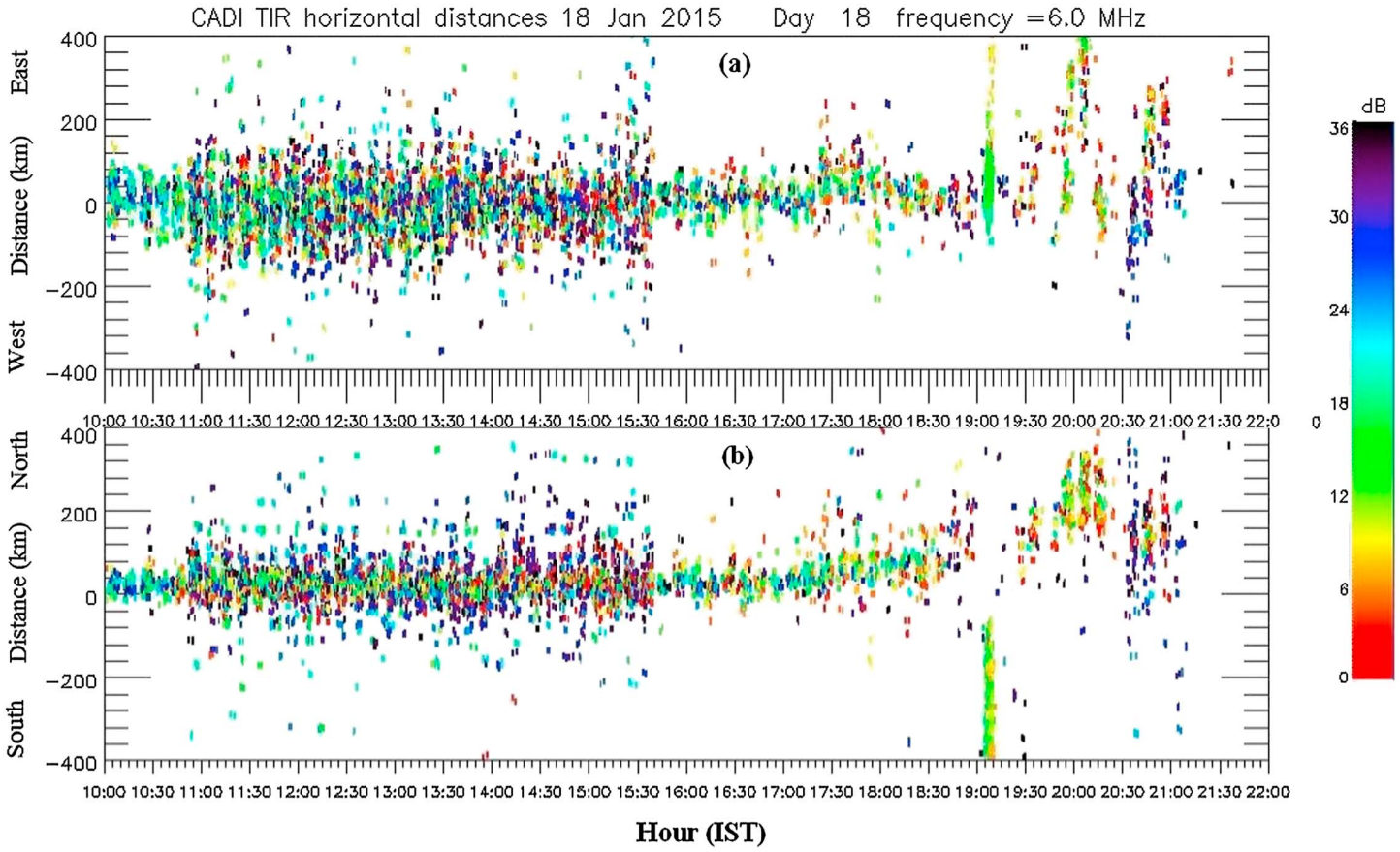


**Figure 3.** (a and b) The east-west and north-south distance of the scatterers at 400 km distance from the ionosonde station as obtained using 6 MHz frequency.

The three-dimensional velocity vector $v$ can be estimated from a collection of source locations defined by $k_s$ and Doppler shifts $d_s$ by minimizing the least squares error [after *Cannon et al.*, 1991].

$$\varepsilon^2 = \sum_s \left( d_s - \frac{1}{\pi} v.k_s \right)^2$$

where $s = 1,2,3\ldots\ldots$(source index).

It may be mentioned that this technique fails when only few number of reflecting sources are available for drift measurements.

Accordingly, we processed the drift data only when enough source points are available.

## 3. Results

In this section, first, we present typical examples of temporal variations in the zonal and vertical drift measurements at Tirunelveli as obtained from CADI system. Then, we present a typical comparison of CADI vertical drifts with same drifts made from digisonde at Trivandrum which is close to the Tirunelveli. Later on, we present seasonal and monthly variations of these drifts during geomagnetically quiet periods. We also present a comparison with drift model of *Scherliess and Fejer* [1999] and drifts from that of *h'f* (km) along with relevant discussions.

### 3.1. Typical Diurnal Variation of Vertical and Horizontal Drifts

Figure 4a shows the typical diurnal variation of ionization layer movement on 18 January 2015 at 4 MHz frequency in the top. Figures 4b–4d show the diurnal variation of three-component drift velocities referred to as zonal, meridional, and vertical drifts from top to bottom, while the bottom most panel shows the

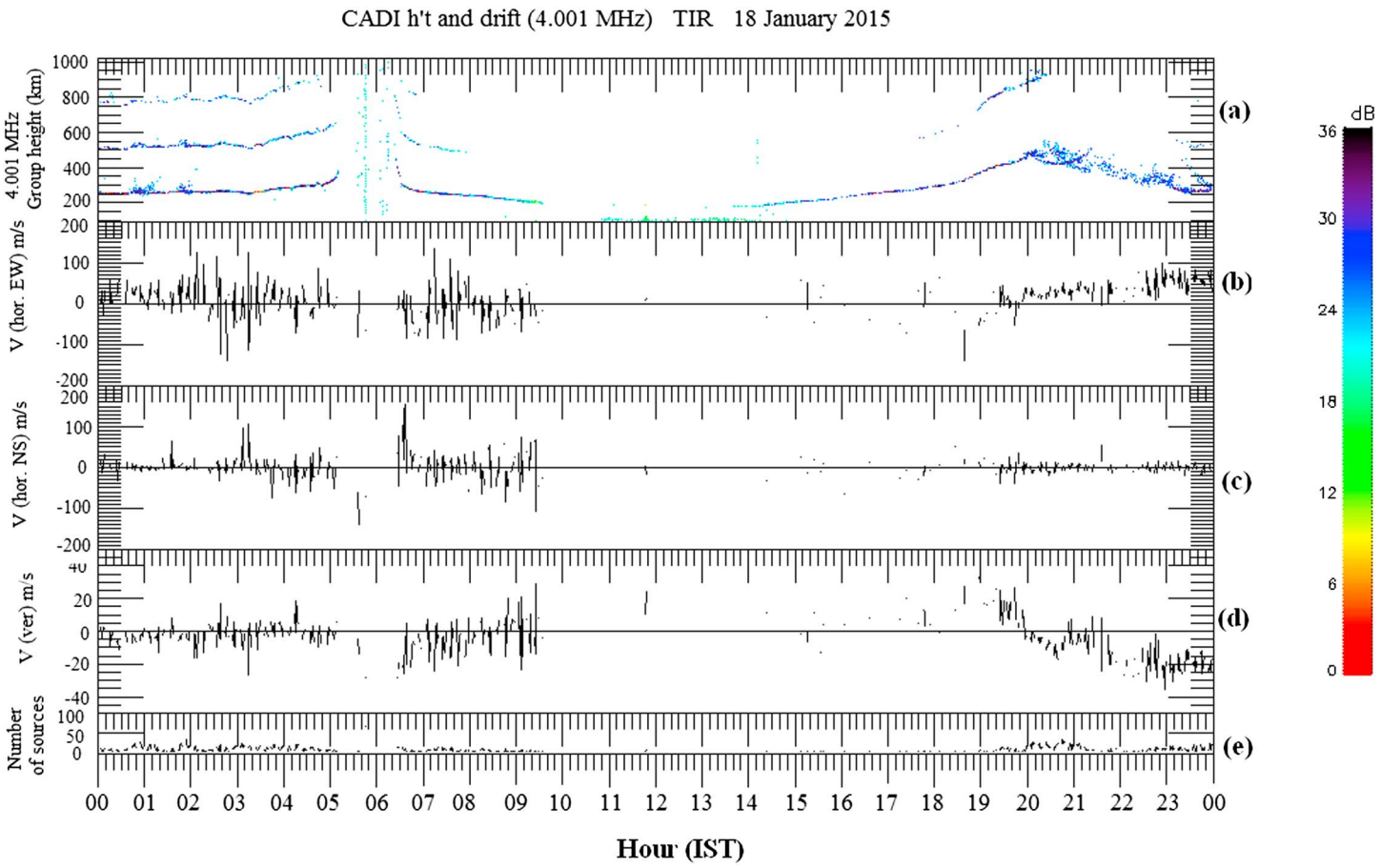


**Figure 4.** (The altitudinal variation of (a) typical ionization layer movement at 4 MHz and its (b) east-west, (c) north-south, (d) vertical drift (m/s), and their scattering sources.

number of scattering sources used for this drift measurement with this frequency. Here it may be mentioned that the threshold of minimum number of scattering sources is 5 to calculate the Drifts. The observations show that during daytime, very few drift measurements were present due to non existence of scattering sources in this frequency, while they show good number of scatterers during nighttimes. While vertical drifts are upward during daytime, it is downward during nighttime. Similarly, zonal drifts are westward during daytime, while they are eastward during night. Meridional drifts are mostly fluctuating about zero during nighttime; they are fluctuating about 50 m/s during early morning hours. Since these irregularities are highly field-aligned, they mostly drift in the zonal direction. So meridional drifts are not really investigated further in this paper.

### 3.2. CADI Vertical Drifts Versus Lowell's DPS Digisonde Vertical Drifts

In order to compare the CADI drifts with Digisonde drifts, a comparison is being made with the vertical drifts from these two ionosondes on a typical day. Figure 5a shows the CADI drifts at Tirunelveli on 06 March 2010, while Figure 5b shows the digisonde (1) base height and (2) drifts on same day at Trivandrum, which is ~100 km away from Tirunelveli site. Since there were discontinuities existing in the drift measurements at individual frequencies, we plotted mean drifts and their standard deviation at frequencies of 3.75 MHz and 5.25 MHz. The digisonde drifts are obtained from the published result of *Thampi et al*. [2012] for comparison purpose only. Initially, the drifts were 20 m/s in the CADI, then the drifts go down and again it went upto 40 m/s at 19:45 IST (Indian Standard Time). But again, the drifts slowly went down close to zero and continued until 21:30 IST. Again, the drifts went up for some time and reached 10 m/s before it again reverses its direction. The −ve drift is continued until 00:00 IST. On the other hand, DPS drifts show initially 15 m/s and then rise to 20 m/s at 19:00 IST. This continued until 20:30 IST. Though there were small differences existing between these two drifts which could be due to distance between these two systems, the comparison

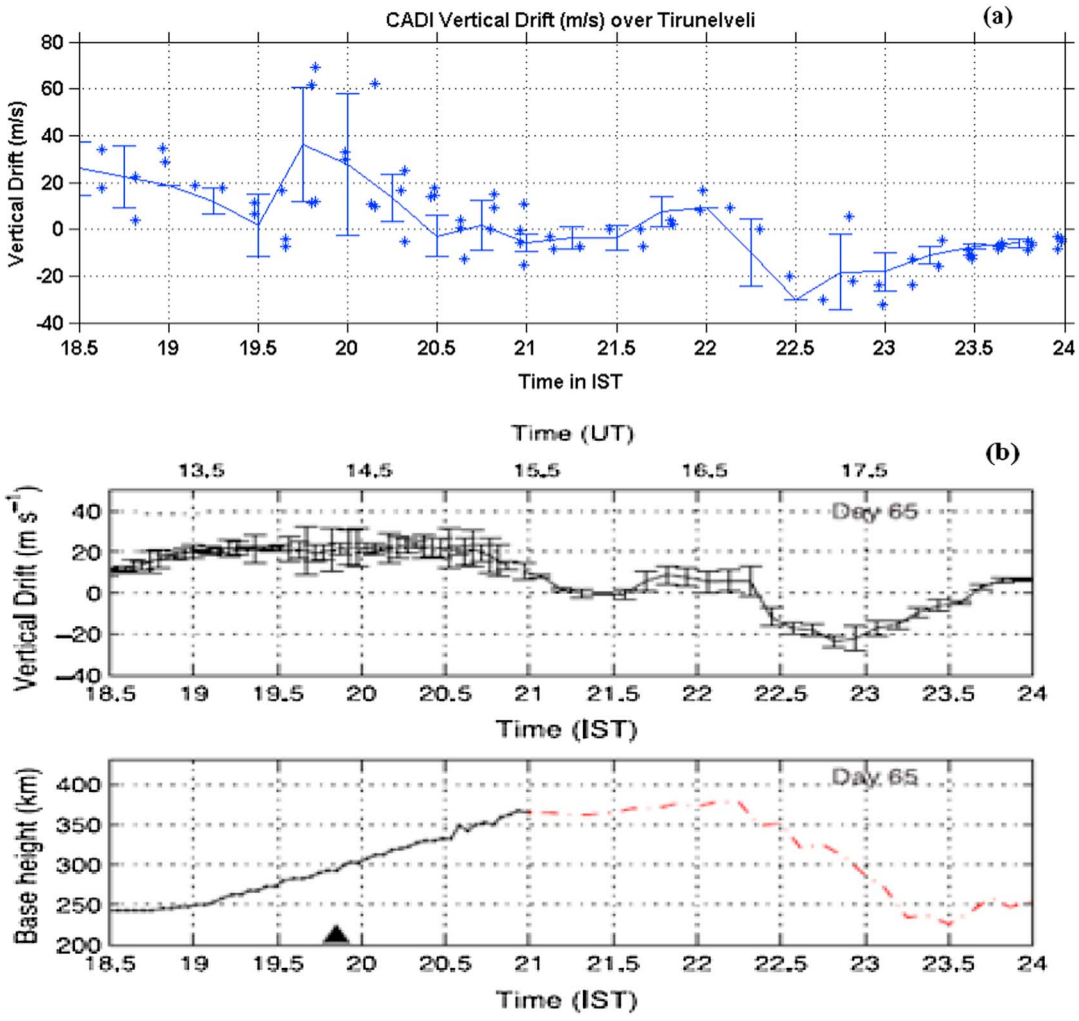


**Figure 5.** (a and b) The comparison of CADI drifts at Tirunelveli with that of digisonde drifts at Trivandrum on same day which is ~100 km away from Tirunelveli.

showed that the trends were in good agreement with each other. This suggests that we can use CADI drifts reliably when electrodynamics dominates.

### 3.3. Monthly Variation of Quiet Time Vertical and Zonal Drifts

After having compared the drifts from independent and proven systems like digisonde, we analyzed quiet time drifts by using larger period of data to study the temporal variation of these drifts and their seasonal behavior. Figures 6a–6l show the scatterplot of the monthly diurnal variation of quiet time vertical drifts over Tirunelveli from January to December 2012 in each individual subplot as obtained by using the frequencies of 4 and 5 MHz. The mean solar flux varied between 93 (min) to 126 (max) solar flux unit (sfu) during this period. The monthly mean drift from Scherliess and Fejer (SF) drift model for each month after taking actual solar flux values into this model (green) is also shown. The observations show that while daytime drifts are upward, during nighttime, these drifts are downward. It may be noted that daytime drift measurements are contaminated by photoionization [*Abdu et al*., 2003b]. So our motive in this paper is not to discuss about daytime vertical drifts. While we present here daytime vertical drifts as well for brevity, however, a detailed study on daytime vertical drifts and their possible corrections are investigated in a separate paper by *Joshi and Sripathi* [2016]. We present here drifts during evening hours when photoionization is minimum. In the evening hours, the Doppler drifts show strong upward movement, which is due to prereversal enhancement (PRE) in the zonal electric field. These evening drifts are found to show seasonal and day-to-day variability where they are found to have higher drifts during equinox months followed by winter months. On the other hand, summer months have least vertical drifts

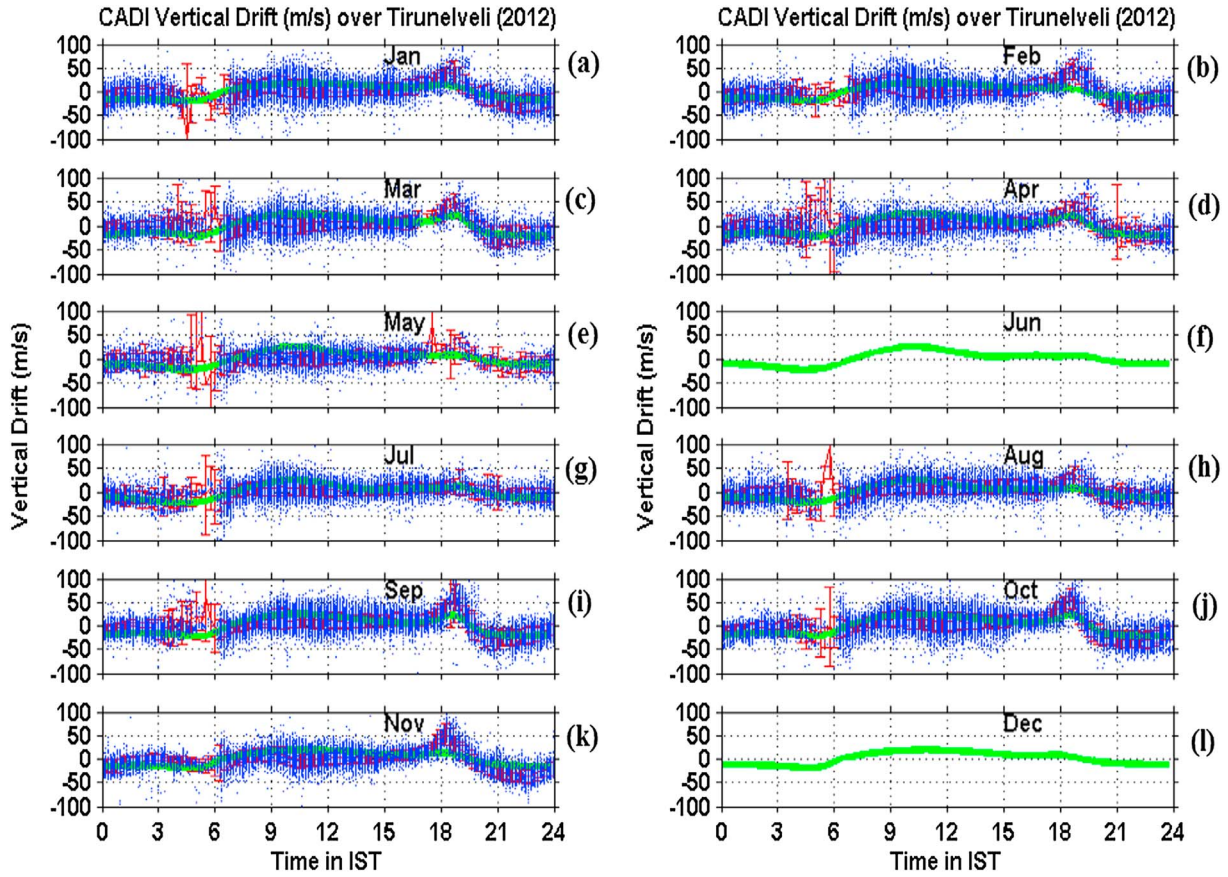


**Figure 6.** (a–l) The scatterplot of the monthly diurnal variation of quiet time vertical drifts over Tirunelveli from January to December 2012 in each individual subplot as obtained by using the frequencies of 4 and 5 MHz. The monthly mean vertical drifts along with its standard deviation shown in red color are also superposed. The monthly mean vertical drift from the drift model shown in green color for comparison is also shown.

during evening hours. While diurnal variation of CADI drifts shows that nighttime drifts are downward with ~20 m/s, daytime drifts are upward drifts with mean drifts of ~10–15 m/s. In the evening hours, the PRE drifts vary from 30 to 50 m/s. Notable points from this figure are that (a) model calculations do not reproduce actual PRE vertical drifts during evening hours and (b) higher estimation of morning vertical drifts during 08:00–12:00 in the model than CADI drifts. There are also some fluctuations in the vertical drifts during early morning hours, which could be due to lack of scatterers during that time. It seems the Doppler vertical drifts obtained from CADI underestimate daytime drifts in comparison to model drifts. This could be due to the fact that CADI drift measurements are made by using low number of scattering sources.

Figures 7a–7l show the scatterplot of monthly diurnal variation of quiet time zonal drifts over Tirunelveli from January to December 2012 in each individual subplot as obtained by using the drifts from both frequencies of 4 and 5 MHz. This is done to minimize the data gaps. Due to not having the data during June and December, the panels look blank. The observations show that daytime zonal drifts are westward with mean drifts varying about 150 m/s, while these drifts are eastward during nighttime with mean drifts varying about 100 m/s. In the evening hours, however, there is a large westward movement in the drifts which could be linked to the upward drift due to prereversal enhancement (PRE) in the zonal electric field. The drifts are found to show lower drifts during daytime during summer months as compared to other months. On the other hand, summer months have least vertical drifts during evening hours. The zonal drifts in the nighttime shows that they also show variability where autumn equinox period seems to have higher zonal drifts in comparison to other periods.

### 3.4. Doppler Drifts Versus Drifts From Virtual Height Versus SF Drift Model

When Doppler drift measurements were not available, we usually use virtual height (km) of *F* layer to calculate vertical drifts by using the rate of change of layer height after assuming that there is no production and

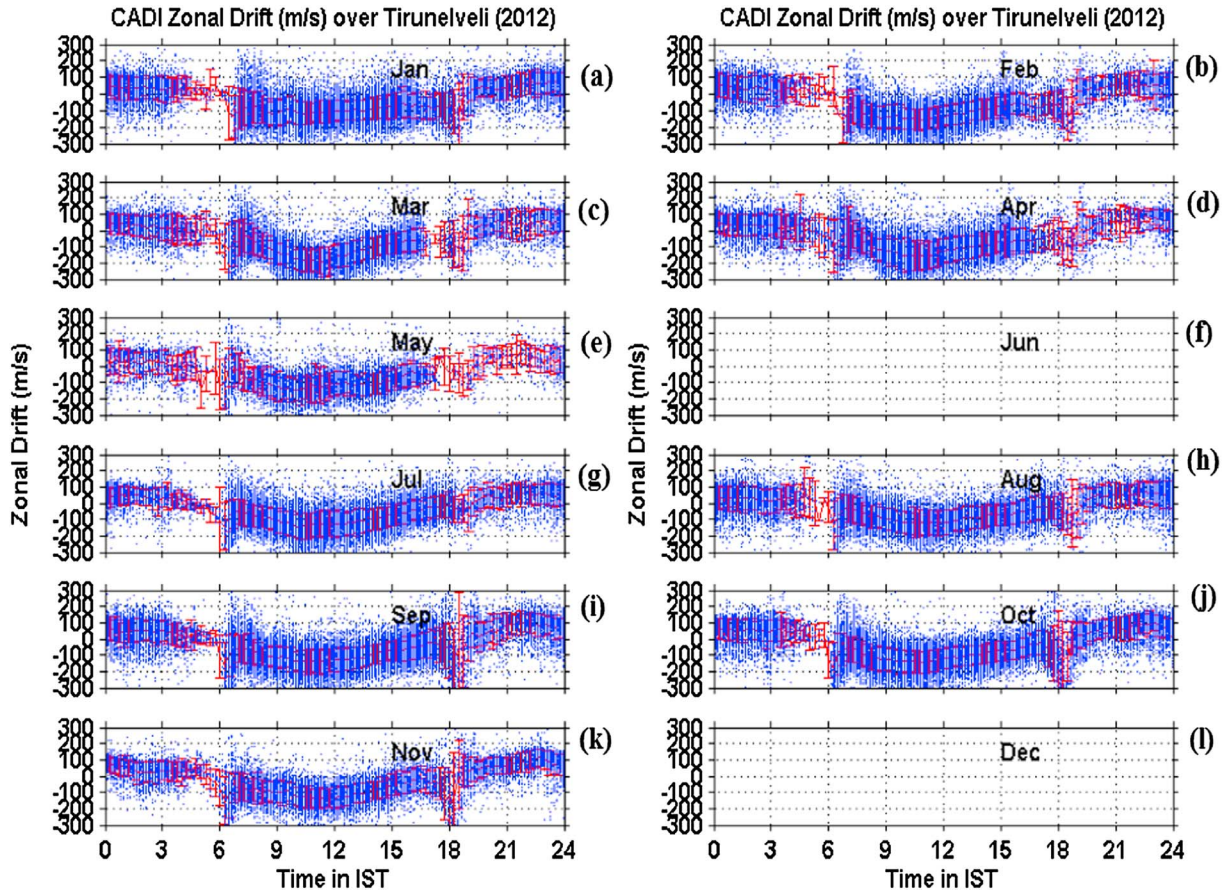


**Figure 7.** (a–l) The scatterplot of monthly diurnal variation of quiet time zonal drifts from January to December 2012 as shown in each individual subplot obtained by using the mean of the drifts between frequencies 4 and 5 MHz. The monthly mean zonal drifts along with its standard deviation shown in red color are also superposed.

negligible recombination of ionization after sunset. Since now we have measured the drifts by using Doppler method, it is possible to compare these two methods. In order to compare the drifts measured by using Doppler drift technique with virtual height method and SF model, we plotted the contour map of daily temporal variation of vertical drifts obtained by using Doppler drifts, drifts obtained by using virtual height measurements and SF model drifts during 18:00–00:00 IST in Figures 8b–8d, respectively. It may be noted that we manually scaled the virtual height at 4 MHz frequency to obtain drifts. In the virtual height method, the drifts are obtained by using the rate of change of layer height with time when no production or recombination takes place. These drifts are used extensively for drift measurements [e.g., *Jayachandran et al*., 1993]. The contour map of day-to-day variations in the zonal drifts shown in Figure 8a is also plotted. The observations show clearly the enhancement of vertical drifts during evening hours in both methods. This suggests that we can use CADI Doppler drift measurements to understand the dynamics of the equator. The observations also suggest that these drifts have strong seasonal variation where they show that equinox has higher vertical drifts than other seasons. Detailed look at the observations suggests that, in addition, these drifts also show equinoctial asymmetry in their drifts where it is found that autumn equinox has higher vertical drifts than that of vernal equinox. Since similar equinoctial asymmetry in PRE is observed independently from both Doppler drift technique and from the rate of change of virtual height method, the Doppler drift method seems reproducing the drifts properly. Also, such asymmetry is noticed in the zonal drifts as can been in Figure 8a. To study the daily variation of Doppler drifts and drifts from virtual height at different times in the post sunset hours, we have plotted the daily variation of these drifts in Figures 9a and 9b. It shows very clearly that the trends are quite similar in both methods, though Doppler drifts are showing bit higher drifts. In order to correlate the Doppler drifts with drifts from virtual height and SF model, we have plotted the correlations between them in Figures 10a and 10b. Figure 10a shows the correlation of Doppler drifts with drifts

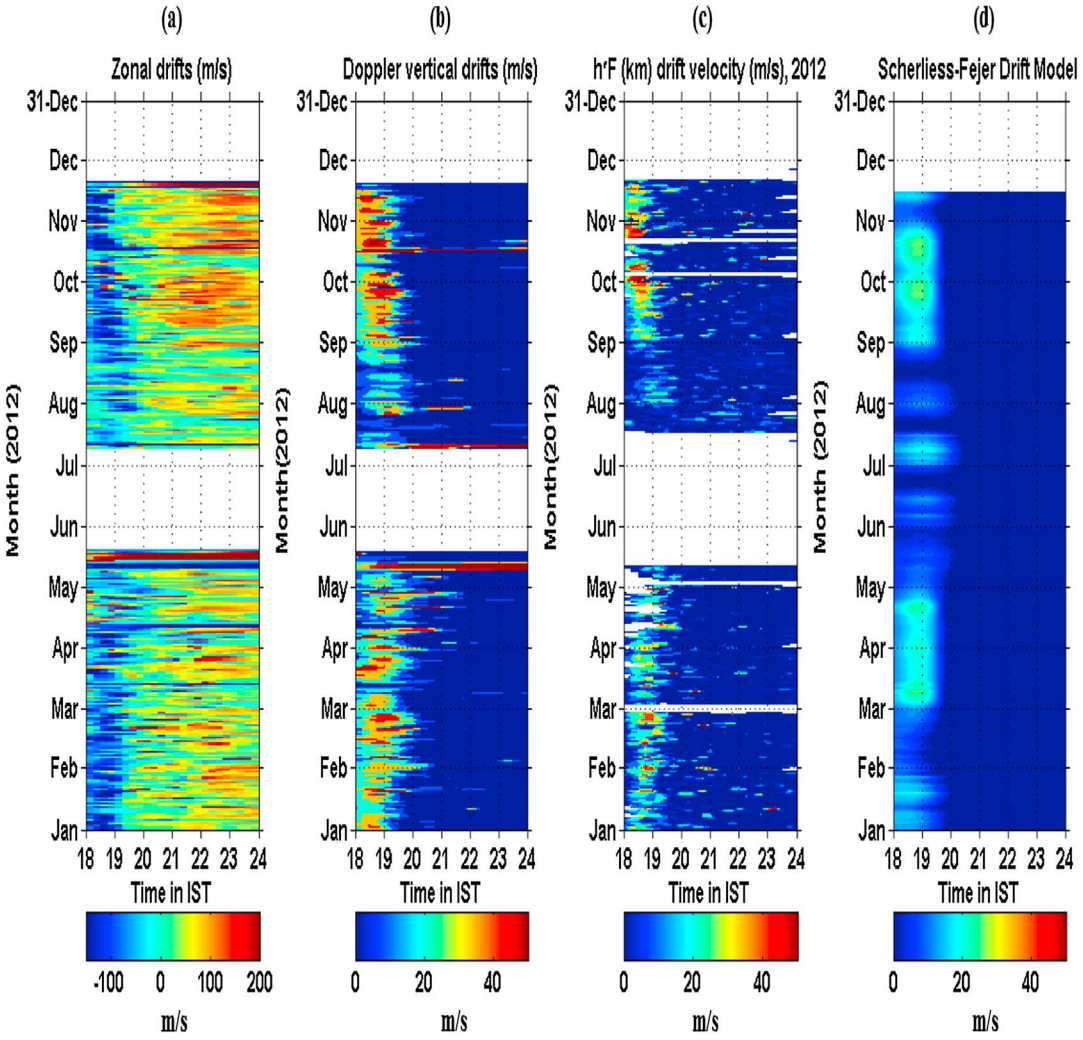


**Figure 8.** The contour map of daily temporal variation of (a) zonal drifts. (b and c) The vertical drifts obtained by using Doppler drift measurements and drifts obtained by using virtual height measurement at 4 MHz, respectively. (d) The SF drift model for comparison is also shown. The white gap in all the plots represents the data gap.

obtained by using virtual height (km), while Figure 10b shows the correlation between Doppler drifts and drifts obtained by using SF model using daily drifts at 18:30 IST. The correlation coefficient shows that while the Doppler drifts correlate with that of the drifts obtained by using virtual height to a reasonable extent, however, the SF model drifts show saturation at higher velocities when it is compared with Doppler drifts.

Since daytime is believed to be driven by *E* region processes due to high conductivity, we studied the correlation of zonal drifts with EEJ strength at different times during daytime. The correlation plots are shown in Figures 11a–11d for different times. *Woodman et al*. [2006] have shown that daytime drifts are influenced by primary kilometer-scale EEJ irregularities. The correlation plot suggests that they have good correlation at different times but slopes are negative. When we calculated the correlation coefficient (*R*) between them, the correlation coefficient is found to be on the order of 0.5 to 0.63 at different times with negative slopes indicating that they are negatively correlated; i.e., zonal drifts are eastward (westward) when EEJ strength is less (more). However, it may be mentioned that further study is needed because the daytime Doppler drift velocity may be poor now.

### 3.5. Day-to-Day Variability in Spread *F* Occurrence/L-Band Scintillations (2012)

In order to relate the drift velocities presented above with spread *F* occurrence or GPS L-band scintillations, we have studied the spread *F* occurrence or GPS L-band scintillations in Figures 12a–12c. The panels in the

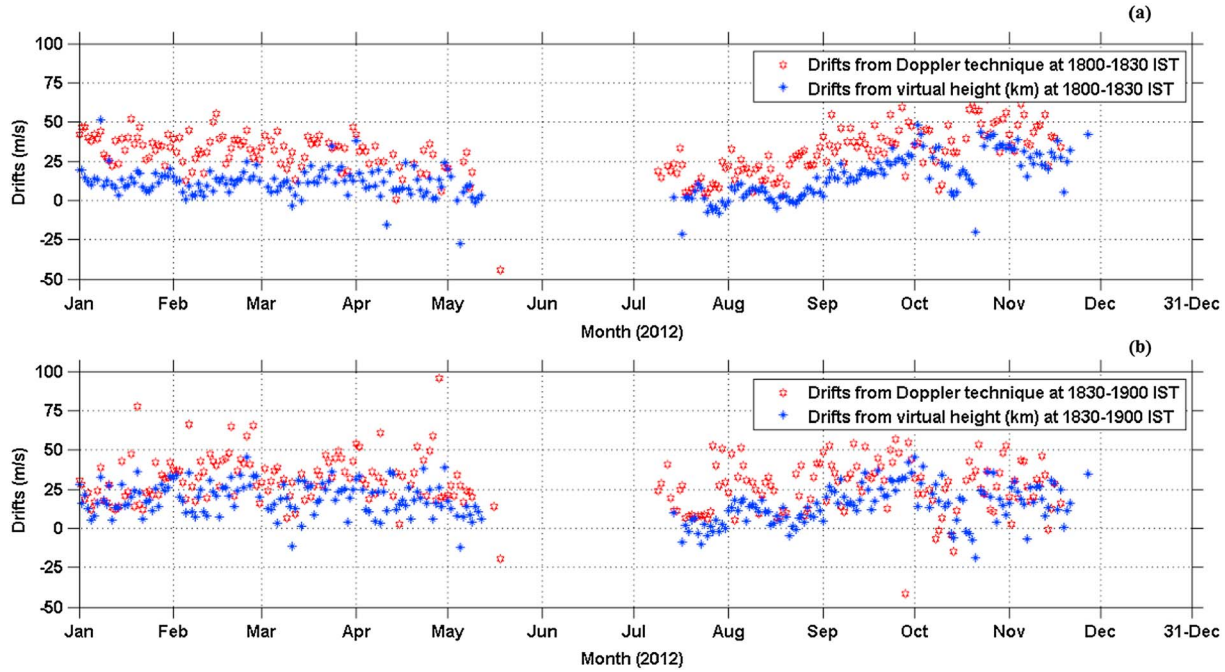


**Figure 9.** The comparison of variation of mean Doppler drift and the drifts obtained by using virtual height (km) at 4 MHz at (a) 18:00–18:30 IST and (b) 18:30–19:00 IST during evening PRE times.

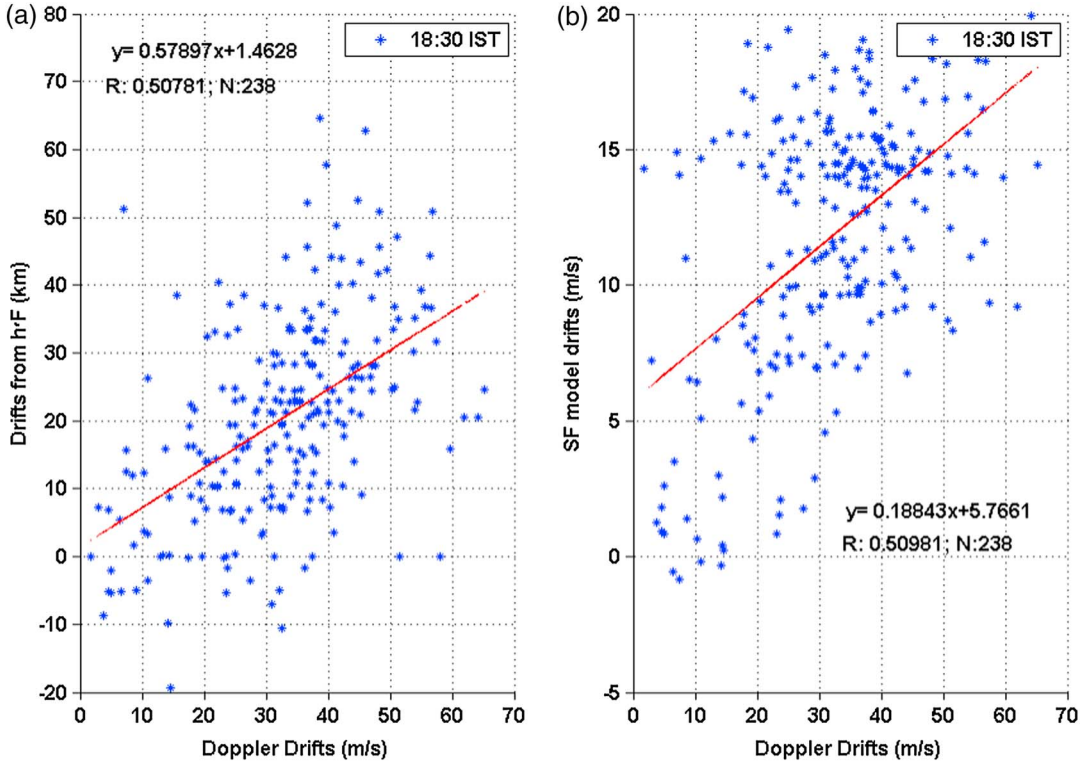


**Figure 10.** (a and b) The correlation of Doppler drifts with drifts obtained by using virtual height (km) and drifts obtained by using Scherliess and Fejer (SF) model using daily drifts at 18:30 IST.

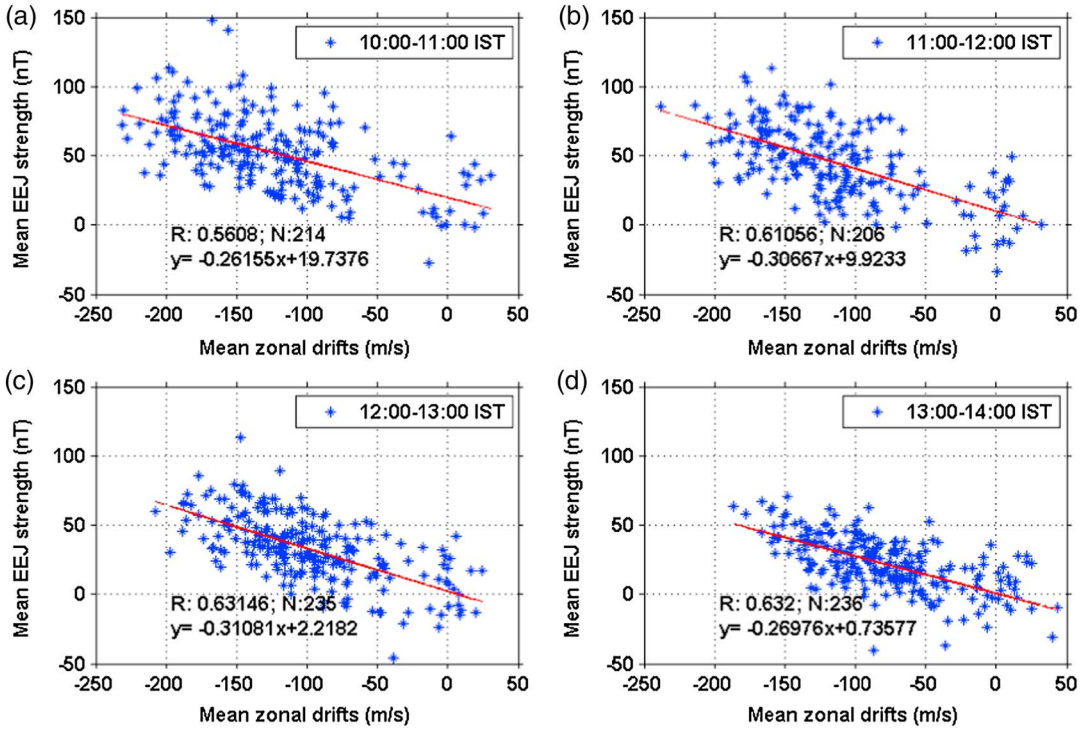


**Figure 11.** (a–d) The correlation of zonal drifts with EEJ strength at different times during daytime.

figure from top to bottom show the daily variation of (a) monthly solar flux, (b) L-band scintillations, and (c) occurrence duration of spread *F* irregularities in ionograms over Tirunelveli for the year 2012. While gaps in the bottom two panels show the data gap. The observations show that spread *F*/scintillations are strong when drifts are strong. These observations show that spread *F*/scintillations are strong during equinox periods. However, these observations also show equinoctial asymmetry in their occurrence where occurrence of spread *F* is more during autumn equinox than vernal equinox. However, this equinoctial asymmetry is different from the usual asymmetry reported in the literature where occurrence of irregularities/scintillations is seen more during vernal equinox than autumn equinox [e.g., *Sripathi et al*., 2011, and references therein]. In addition, the observations also show early occurrence of spread *F*/scintillations during autumn equinox than vernal equinox.

## 4. Discussions

The equatorial vertical and zonal drifts over Tirunelveli presented above show the following characteristics: (a) enhancement of vertical drifts during PRE times, (b) westward zonal drifts during daytime and eastward drifts during nighttime, (c) good correlation between EEJ and daytime zonal drifts, (d) higher Doppler drifts than *h′f* (km) method and SF model drifts, (e) seasonal variation of vertical drifts in the evening hours wherein equinox has larger vertical drifts followed by winter and summer, (f) the vertical drifts are also having equinoctial asymmetry where autumn equinox sees higher vertical drifts than vernal equinox which is in association with spread *F* and L-band scintillation observations, and (g) shears in the zonal drift prior to ESF onset. Higher Doppler vertical drifts as seen here could possibly be due to high sampling (~1 min) of Doppler drifts, which measures individual scattering points. However, in the virtual height (km) method, we are measuring average drift velocity of the ionization layer, which is the average drift. Because of this difference, possibly, we are getting higher Doppler drifts than virtual height method. Other possibility is the number of scattering points that go for drift estimates in CADI. We had a threshold of five scattering points above which we considered as a signal. Unlike DPS system, CADI system does not receive more scattering points. However, when we compared both of them, even though CADI system does not have more number of scattering points still we could get better estimates of the drifts. So we believe that may be due to

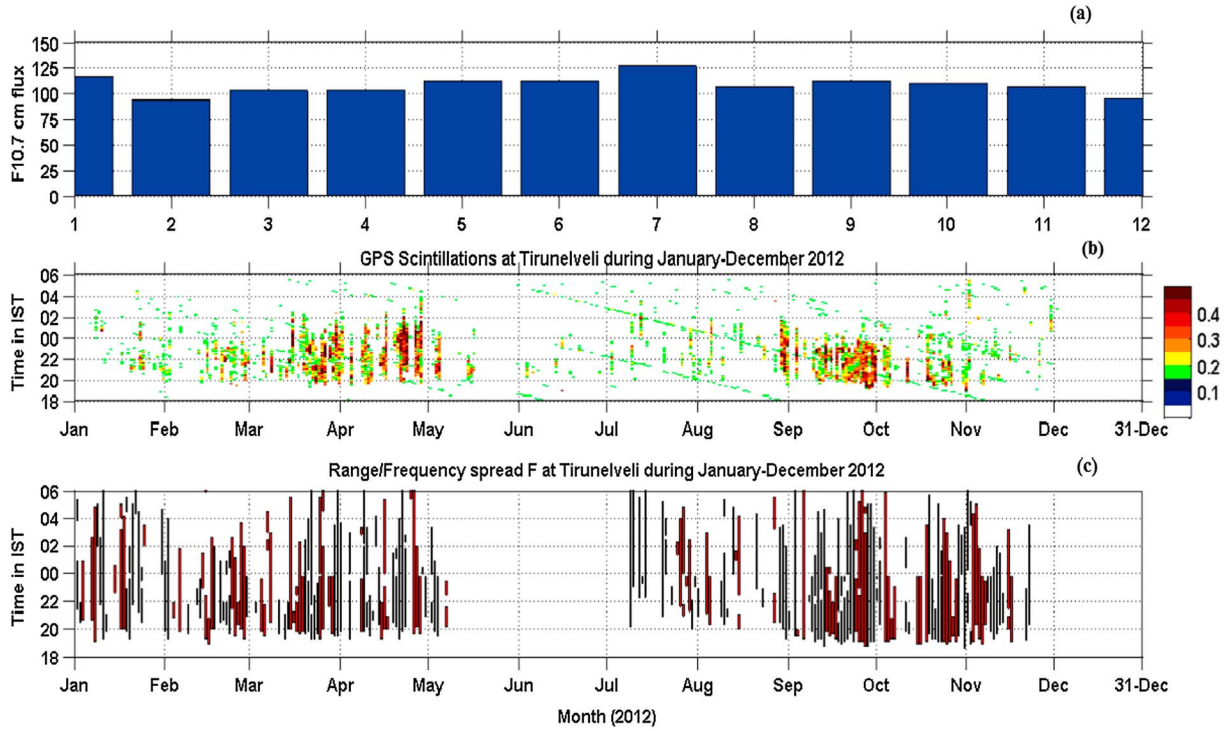


**Figure 12.** The daily variation of (a) monthly solar flux, (b) L-band scintillations (S4 index), and (c) occurrence duration of spread *F* irregularities in ionograms over Tirunelveli for the year 2012. The white gap in the bottom two panels represent the data gap.

different resolutions of Doppler drifts and virtual height (km), respectively, we are getting higher drifts in Doppler drifts. On the other hand, *Kouba and Knížová* [2012] investigated digisonde drift data with larger data over midlatitude station Pruhonice and suggested that Doppler drifts do provide valuable information about ionospheric drifts even at the time of low number of scattering sources. While keeping the importance of valuable information this system can provide, we have investigated the drifts in a detailed manner.

*Namboothiri et al.* [1989] have studied the diurnal variation of vertical drifts by using HF radar over Trivandrum and showed that they are upward during daytime, higher vertical drifts during PRE periods and downward during nighttime. They further showed that drifts during PRE period vary as per solar flux, season, and magnetic activity levels. Since we do not have other long-term drift data, we could not check the solar flux variation. During the year 2012, solar flux is almost constant during equinoxes and winter season, however, with higher flux values during summer season. The mean solar flux varied between 93 (min) sfu during equinox to 126 (max) sfu during summer during the period under consideration in this paper (see Figure 10a for details). *Subbarao and Krishnamurthy* [1994] have also studied the post sunset *F* region vertical drifts and suggested that there is a quasiperiodic fluctuation in the vertical drifts with periods in the range of 4–30 min superposed on a steady vertical drift. They attributed these fluctuations to internal gravity waves which are needed for spread *F* occurrence. Closer look at the observations suggests that we do see such oscillations in our vertical drifts; however, we will investigate these small-scale variations exclusively in another work. Using HF Doppler radar, height gradient in the vertical drifts is studied over Indian region [*Sastri et al*., 1995; *Prabhakaran Nayar and Sreehari*, 2004]. They suggested that positive height gradient of vertical drifts below the *F* layer peak may be suggestive of altitude dependence of relative contributions of *E* and *F* region dynamos to the electric fields responsible for variations in the plasma drifts.

The vertical and zonal drift velocities obtained by using Doppler drift technique of digisonde are compared with co-located incoherent scatter radar over Jicamarca [*Bertoni et al*., 2006; *Woodman et al*., 2006]. *Bertoni et al*. [2006] have shown that digisonde drifts are in agreement with incoherent scatter radar (ISR) drifts during evening hours (until 22:00 LT). Also, their drifts are in good agreement with ISR drifts during postmidnight, sunrise, and magnetically disturbed periods when bottomside *F* layer is above ~300 km height. They suggested that vertical drift velocities measured by digisondes are reliable for studies of ionospheric phenomena

during sunset and evening hours and also during some late night and sunrise hours as well as during magnetically disturbed events. They have noticed consistent differences between the ISR and digisonde vertical drift on some daytime occasions, which they interpreted to be due to the photochemistry that affects the refractive index along the path of the HF radio waves. On the other hand, *Woodman et al*. [2006] have shown that digisonde vertical drifts showed good agreement with ISR drifts whenever PRE dominates. However, they suggested that while vertical drifts could be contaminated by production or recombination during daytime, *F* region zonal drifts can be used when the *F* region is structured and the *E* region density is low. Further, they have shown that the daytime zonal drifts as obtained from their ionosonde could be driven by zonal kilometer-scale EEJ irregularities over equator. As a result, they suggested that during daytime only *E* region zonal drifts and not *F* region zonal drifts are obtained. Now since we do not have simultaneous radar observations to check daytime *E* region drifts and their correlation to ionosonde zonal drifts to prove that EEJ irregularities are responsible for zonal drifts, we tried to compare our zonal drifts with EEJ strength as EEJ can be used as a proxy for EEJ irregularities. Our comparison showed good correlation with EEJ strength, suggesting that these zonal drifts are indeed driven by *E* region processes when *E* region is dominant. It also may be noted that there is a report that mesosphere-lower thermosphere (MLT) region winds are contaminated in MF radar observations due to *E* region plasma irregularities [*Ramkumar et al*., 2010]. They showed that zonal drifts of 100–200 m/s in the MLT region could be due to *E* region plasma irregularities. *Tiwari et al*. [2003] have compared the Doppler drift velocities by using simultaneous HF and VHF observations over Trivandrum and suggested that Doppler velocities could be on the order of 150–200 m/s in the *E* region, which is in agreement with our zonal drifts. Further, they showed that these drift velocities are scale size-dependant, which means that drift varies with scale size of the probing wavelength. Similarly, using spaced receiver VHF scintillation measurements, recently, *Yadav et al*. [2015] have shown that zonal drifts are having drift speeds on the order of 120 m/s. On the other hand, the temporal variations of zonal drifts also suggest higher eastward drifts during evening hours at PRE times, while they show slow reduction of these drifts to westward in the late nights. Interestingly, zonal drifts also show its higher eastward drifts during autumn equinox when vertical drifts also show higher vertical drifts. *Bhattacharyya et al*. [2001], on the other hand, have shown the eastward drifts by using spaced receiver scintillation technique. They have shown that while eastward drifts reach the maximum of 200 m/s during 20:00 LT, later these drifts slowly reduces to 100 m/s at about midnight sector. Using optical observations of plasma plume in airglow, *Taori and Sindhya* [2014] have calculated the nighttime zonal drifts. Their drifts do suggest that nighttime zonal drifts increase to 150 m/s at 20:00 LT over Indian region. *Fejer et al*. [1991] have studied the *F* region zonal drifts by using Jicamarca incoherent scatter Radar in South American region. They have shown that zonal drifts are westward during daytime, while they are eastward during night. Further, they have shown that the zonal drifts do not vary with season, solar flux, and magnetic activity during daytime. However, they have shown that *F* region zonal drifts vary with solar flux and magnetic activity during evening hours and nighttime. Previous studies over Indian region have shown that *F* region exhibits altitude variation around dusk sector where lower altitudes show westward and higher altitudes show eastward. Due to this altitude variation, zonal shears are generated, which are important for spread *F* onset. The observations presented here also suggest that zonal drifts are westward during daytime and they do not vary with season and local time during daytime, which is in accordance with observations of *Fejer et al*. [1991]. However, in the nighttime, they move eastward with mean velocity of ~100 m/s in the premidnight period and then reduces slowly in the postmidnight period, which follows the trend as per the earlier observations. Also, our observations suggest that there is a strong variability of the zonal drifts around dusk sector, which seems to vary with season. The observations presented in this paper suggest that due to variability in the zonal drifts, zonal shears are produced, which is required for spread *F* onset. When we compared these zonal shears during different seasons, it is seen that this shears are more during autumn equinox than vernal equinox, which could be providing more favorable conditions for the spread *F* onset, which may be one of the reasons for having strong spread *F*/scintillations in the autumn equinox than vernal equinox.

Recently, *Patra et al*. [2014a] have compared the vertical drifts obtained by using 150 km echoes at Gadanki and C/NOFS ion drift measurements and suggested that 150 km echoes do represent vertical drifts during daytime. In fact they also compared their drifts with EEJ strength on monthly basis and found that they are in good agreement [*Patra et al*., 2014b]. While their drifts are comparable to C/NOFS ion drifts in magnitude, however, SF drift model could not reproduce these drifts when drifts are either lower or higher. Also, day-to-day variations in the drifts could not be comparable to that of C/NOFS drifts. They also suggested that

reason for this variation on day-to-day basis is due to differences in probing volume with which these instruments are sensing where there could be variations in thermospheric tides and gravity waves. Our observations suggest that SF model drifts are lower as compared to Drift model. Due to large day-to-day variability and due to different modes of operation, our results may be showing poor correlations. Using $h_mF_2$ method, *Oyekola et al*. [2007] have also studied the vertical drifts over African region by using ionosonde. They showed that their PRE drift variations are in good agreement with solar flux variations. More recently *Joshi and Sripathi* [2016] have studied the daytime vertical drifts by using ionosonde, and a correction factor is being identified and is applied based on neural network technique. These drifts were also compared with C/NOFS ion drifts and EEJ strength. The correlation is reasonably in good agreement with satellite drift measurements. Using vertical and zonal drifts in the evening hours as measured by using HF Doppler radar, it is shown that it is possible to study the plasma vortex in the evening ionosphere, which is believed to be responsible for the generation of ESF onset [*Sreehari et al*., 2006; *Mathew and Nayar*, 2012]. So our observations of higher variations of zonal drifts at the time of PRE time indicate that plasma vortex indeed existed at this time. However, we need to examine the altitude structure to examine it. It may be pointed out that we have seen higher scintillations during autumn equinox during the same year, which could be believed to be due to combination of higher vertical drifts and shears in zonal drifts during this period. So the observations presented here suggest that CADI does reproduce the drifts at Indian low latitudes and may be used effectively to study the electrodynamics of the low latitudes.

## 5. Concluding Remarks

We presented temporal and seasonal characteristics of quiet time vertical and zonal drifts by using Doppler interferometry technique using Canadian ionosonde at Tirunelveli. The observations suggest that seasonal variations of evening hour vertical drifts are high during equinox followed by winter and summer, respectively. However, there exists an equinoctial asymmetry in the drifts where in autumn equinox sees higher drifts which are in agreement with spread *F* or L-band scintillations. The vertical drifts so obtained are compared with digisonde drifts at Trivandrum, SF model, and drifts calculated by using virtual height. Case study presented here showed that the CADI drifts are able to reproduce digisonde drifts with comparable magnitude. On the other hand, the drifts calculated by using Doppler drift technique showed reasonable agreement with drift measurements made by using drifts obtained from virtual height in terms of trends. However, the drifts calculated by using virtual height and SF model appear to be relatively low. On the other hand, the zonal drifts are found to be westward during daytime with mean drifts of 150–200 m/s and are negatively correlated to the EEJ strength, indicating that they are driven by *E* region dynamo, while they are eastward during nighttime with mean drift magnitude of 100 m/s, which are in agreement with *F* region dynamo. The eastward drifts are also found to rise to its maximum velocities at about 20:00 LT prior to its gradual reduction. The zonal drift velocities as obtained here are comparable with same drifts measured over Indian region by using other techniques. The zonal drifts presented here are relatively higher during autumn equinox prior to PRE period than vernal equinox when strong ESF irregularities are present indicating that zonal drifts also may be playing its role in ESF onset. Hence, based on these observed results, it suggests that CADI Doppler drifts obtained at Tirunelveli indeed can be used for routine drift measurements that are relevant for understanding the variable ionosphere over Indian longitudes.

**Acknowledgments**

The research work presented here is carried out through the funds from in-house project at IIG (DST), Government of India. The technical staff at EGRL is highly acknowledged for their constant support in operating and maintaining the CADI ionosonde system. Authors would like to thank the director of IIG for kind support and encouragement. We also would like to acknowledge M.A. Abdu, INPE, Brazil, for his expert suggestions or discussions. Part of this work is done at International Centre for Theoretical Physics (ICTP), Italy, when the lead author (S.S.) was at ICTP under its associateship program. S.S. would like to thank Sandro Radicella at Aeronomy Laboratory at ICTP for extending his kind support. The data and figures presented in this paper are with corresponding author (S.S.), and he can be contacted at e-mail: ssripathi.iig@gmail.com.

## References

Abdu, M. A., I. S. Batista, H. Takahashi, J. MacDougall, J. H. Sobral, A. F. Medeiros, and N. B. Trivedi (2003a), Magnetospheric disturbance induced equatorial plasma bubble development and dynamics: A case study in Brazilian sector, *J. Geophys. Res.*, *108*(A12), 1449, doi:10.1029/2002JA009721.

Abdu, M. A., J. W. MacDougall, I. S. Batista, J. H. A. Sobral, and P. T. Jayachandran (2003b), Equatorial evening prereversal electric field enhancement and sporadic E layer disruption: A manifestation of E and F region coupling, *J. Geophys. Res.*, *108*(A6), 1254, doi:10.1029/2002JA009285.

Abdu, M. A., P. T. Jayachandran, J. MacDougall, J. F. Cecile, and J. H. A. Sobral (1998), Equatorial F region zonal plasma irregularity drifts under magnetospheric disturbances, *Geophys. Res. Lett.*, *25*, 4137–4140, doi:10.1029/1998GL900117.

Balan, N., B. Jayachandran, R. B. Nair, S. P. Namboothiri, G. J. Bailey, and P. B. Rao (1992), HF doppler observations of vector plasma drifts in the evening F-region at the magnetic equator, *J. Atmos. Sol. Terr. Phys.*, *54*, 1545–1554, doi:10.1016/0021-9169(92)90162-E.

Bertoni, F., I. S. Batista, M. A. Abdu, B. W. Reinisch, and E. A. Kherani (2006), A comparison of ionospheric vertical drift velocities measured by digisonde and incoherent scatter radar at the magnetic equator, *J. Atmos. Sol. Terr. Phys.*, *68*(6), 669–678, doi:10.1016/j.jastp.2006.01.002.

Bhaneja, P., G. D. Earle, R. L. Bishop, T. W. Bullett, J. Mabie, and R. Redmon (2009), A statistical study of midlatitude spread F at Wallops Island, Virginia, *J. Geophys. Res.*, *114*, A04301, doi:10.1029/2008JA013212.

Bhattacharyya, A., S. Basu, K. M. Groves, C. E. Valladares, and R. Sheehan (2001), Dynamics of equatorial F region irregularities from spaced receiver scintillation observations, *Geophys. Res. Lett.*, *28*(1), 119–122, doi:10.1029/2000GL012288.

Bibl, K., and B. W. Reinisch (1978), The universal digital ionosonde, *Radio Sci.*, *13*, 519–530, doi:10.1029/RS013i003p00519.

Breit, G., and M. A. Tuve (1925), A radio method of estimating the height of the conducting layer, *Nature*, *116*, 357, doi:10.1038/116357a0.

Bianchi, C., and D. Altadill (2005), Ionospheric Doppler measurements by means of HF-radar techniques, *Ann. Geophys.*, *48*, doi:10.4401/ag-3248.

Burke, W. J., L. C. Gentile, C. Y. Huang, C. E. Valladares, and S. Y. Su (2004), Longitudinal variability of equatorial plasma bubbles observed by DMSP and ROCSAT-1, *J. Geophys. Res.*, *109*, A12301, 2004, doi:10.1029/2004JA010583.

Cannon, P. S., B. W. Reinisch, J. Buchau, and T. W. Bullett (1991), Response of the polar cap F region convection direction to changes in the interplanetary magnetic field: Digisonde measurements in northern Greenland, *J. Geophys. Res.*, *96*(A2), 1239–1250.

Davies, K. (1989), *Ionospheric Radio*, vol. 31, pp. 580, Inst. Electr. Eng. Electr. Wave Ser., Peter Peregrinus, London.

de La Beaujardiere, O., et al. (2004), C/NOFS: A mission to forecast scintillations, *J. Atmos. Sol. Terr. Phys.*, *66*, 1573–1591, doi:10.1016/j.jastp.2004.07.030.

Fejer, B. G., and M. C. Kelley (1980), Ionospheric irregularities, *Rev. Geophys. Space Phys.*, *18*, 401, doi:10.1029/RG018i002p00401.

Fejer, B. G., E. R. dePaula, S. A. González, and R. F. Woodman (1991), Average vertical and zonal F region plasma drifts over Jicamarca, *J. Geophys. Res.*, *96*(A8), 13,901–13,906, doi:10.1029/91JA01171.

Fejer, B. G., E. R. dePaula, R. A. Heelis, and W. B. Hanson (1995), Global equatorial ionospheric vertical plasma drifts measured by the AE-E satellite, *J. Geophys. Res.*, *100*(A4), 5769–5776, doi:10.1029/94JA03240.

Grant, I. F., J. W. MacDougall, J. M. Ruohoniemi, W. A. Bristow, G. J. Sofko, J. A. Koehler, D. Danskin, and D. Andr´e (1995), Comparison of plasma flow velocities determined by the ionosonde Doppler drift technique, SuperDARN radars, and patch motion, *Radio Sci.*, *30*, 1537–1549.

Hussey, G. C., C. Haldoupis, B. Alain, J. Delloue, and J. T. Wiensz (2004), Mid-latitude E- region bulk motions inferred from digital ionosonde and HF radar measurements, *Ann. Geophys.*, *22*(11), 3789–3798, doi:10.5194/angeo-22-3789-2004.

Hysell, D., and J. Burcham (1998), Julia radar studies of equatorial spread f, *J. Geophys. Res.*, *103*(A12), 29,155–29,167, doi:10.1029/98JA02655.

Jayachandran, B., N. Balan, P. B. Rao, J. H. Sastri, and G. J. Bailey (1993), HF Doppler and ionosonde observations on the onset conditions of equatorial spread F, *J. Geophys. Res.*, *98*(A8), 13,741–13,750, doi:10.1029/93JA00302.

Joshi, L. M., and S. Sripathi (2016), On the utility of the ionosonde Doppler derived EXB drift during the daytime, *J. Geophys. Res. Space Physics*, *121*, 2795–2811, doi:10.1002/2015JA021971.

Kelley, M. C. (1989), *The Earth's Ionosphere: Plasma Physics and Electrodynamics*, Academic Press, San Diego, Calif.

Kouba, D., and P. K. Knížová (2012), Analysis of digisonde drift measurements quality, *J. Atmos. Sol. Terr. Phys.*, *90*, 212–221, doi:10.1016/j.jastp.2012.05.006.

Kudeki, E., and C. D. Fawcett (1993), High resolution observations of 150 km echoes at Jicamarca, *Geophys. Res. Lett.*, *20*, 1987, doi:10.1029/93GL01256.

MacDougall, J. W., I. F. Grant, and X. Shen (1995), The Canadian Advanced Digital Ionosonde: Design and results in: Report UAG-14: Ionospheric Networks and Stations, World Data Center A for Solar-Terrestrial Physics, 21.

MacDougall, J., M. Abdu, P. Jayachandran, J.-F. Cecile, and I. Batista (1998), Presunrise spread F at Fortaleza, *J. Geophys. Res.*, *103*, 23,415–23,425, doi:10.1029/98JA01949.

Mathew, T. J., and S. R. P. Nayar (2012), Vertical shear at the equatorial F-region ionosphere during post-sunset hours, *Adv. Space Res.*, *49*(8), 1277–1281, doi:10.1016/j.asr.2012.01.011.

Namboothiri, S. P., N. Balan, and P. B. Rao (1989), Vertical plasma drifts in the F-region at the magnetic equator, *J. Geophys. Res.*, *94*(A9), 12,055–12,060, doi:10.1029/JA094iA09p12055.

Narayanan, V. L., S. Sau, S. Gurubaran, K. Shiokawa, N. Balan, K. Emperumal, and S. Sripathi (2014), A statistical study of satellite traces and evolution of equatorial spread F, *Earth Planets Space*, *66*, 160, doi:10.1186/s40623-014-0160-4.

Nayak, C. K., V. Yadav, B. Kakad, S. Sripathi, K. Emperumal, T. K. Pant, A. Bhattacharyya, and S. Jin (2014), Peculiar features of ionospheric $F_3$ layer during prolonged solar minimum (2007–2009), *J. Geophys. Res. Space Physics*, *119*, 8685–8697, doi:10.1002/2014JA020135.

Patra, A. K., et al. (2014a), Vertical ExB drifts from radar and C/NOFS observations in the Indian and Indonesian sectors: Consistency of observations and model, *J. Geophys. Res. Space Physics*, *119*, 3777–3788, doi:10.1002/2013JA019732.

Patra, A. K., P. Pavan Chaitanya, S. Sripathi, and S. Alex (2014b), Ionospheric variability over Indian low latitude linked with the 2009 sudden stratospheric warming, *J. Geophys. Res. Space Physics*, *119*, 4044–4061, doi:10.1002/2014JA019847.

Oyekola, O. S., A. Ojo, J. Akinrimisi, and E. R. dePaula (2007), Seasonal and solar cycle variability in F-region vertical plasma drifts over Ouagadougou, *J. Geophys. Res.*, *112*, A12306, doi:10.1029/2007JA012560.

Prabhakaran Nayar, S. R., and C. V. Sreehari (2004), Investigation of height gradient in vertical plasma drift at equatorial ionosphere using multifrequency HF Doppler radar, *J. Geophys. Res.*, *109*, A12308, doi:10.1029/2004JA010641.

Ramkumar, T. K., S. Gurubaran, R. Rajaram, D. Tiwari, and K. S. Viswanathan (2010), A comparison study of zonal drift velocities measurements as seen by MF spaced antenna and HF Doppler radar in the Indian dip equatorial mesospheric and lower thermospheric (80–100 km) region, *J. Geophys. Res.*, *115*, A02306, doi:10.1029/2009JA014728.

Reddi, C. R., M. S. S. R. K. N. Sarma, and K. Niranjan (2009), HF Doppler radar observations of low-latitude spread F, *Radio Sci.*, *44*, RS3003, doi:10.1029/2007RS003777.

Reinisch, B. W. (1996), Modern ionosondes, in *Modern Ionospheric Science*, edited by H. Kohl, R. Rüster, and K. Schlegel, pp. 440–458, Eur. Geophys. Soc., Katlenburg-Lindau, Germany.

Reinisch, B. W., J. L. Scali, and D. M. Haines (1998), Ionospheric drift measurements with ionosondes, *Ann. Geophys.*, *41*(5–6), 695–702.

Reinisch, B. W., M. Abdu, I. Batista, G. S. Sales, G. Khmyrov, T. A. Bullett, J. Chau, and V. Rios (2004), Multistation digisonde observations of equatorial spread F in South America, *Ann. Geophys.*, *22*, 3145–3153, doi:10.5194/angeo-22-3145-2004.

Sastri, J. H., V. K. Varma, and S. R. Nayar (1995), Height gradient of F region vertical drift in the evening equatorial ionosphere, *Geophys. Res. Lett.*, *22*(19), 2645–2648, doi:10.1029/95GL02668.

Scherliess, L., and B. G. Fejer (1999), Radar and satellite global equatorial F region vertical drift model, *J. Geophys. Res.*, *104*(A4), 6829–6842, doi:10.1029/1999JA900025.

Sreehari, C. V., C. Bhuvanendran, and S. P. Nayar (2006), HF Doppler radar observations of vertical and zonal plasma drifts—Signature of a plasma velocity vortex in evening F-region, *Indian J. Radio Space Phys.*, *35*(4), 242.

Sripathi, S., B. Kakad, and A. Bhattacharyya (2011), Study of equinoctial asymmetry in the equatorial spread F (ESF) irregularities over Indian region using multi-instrument observations in the descending phase of solar cycle 23, *J. Geophys. Res.*, *116*, A11302, doi:10.1029/2011JA016625.

Su, S.-Y., H. C. Yeh, and R. A. Heelis (2001), ROCSAT 1 ionospheric plasma and electrodynamics instrument observations of equatorial spread F: An early transitional scale result, *J. Geophys. Res.*, *106*(A12), 29,153, doi:10.1029/2001JA900109.

Subbarao, K. S. V., and B. V. K. Krishnamurthy (1994), Posts-unset *F*-region vertical velocity variations at magnetic equator, *J. Atmos. Terr. Phys.*, *56*, 59.

Taori, A., and A. Sindhya (2014), Measurements of equatorial plasma depletion velocity using 630 nm airglow imaging over a low-latitude Indian station, *J. Geophys. Res. Space Physics*, *119*, 396–401, doi:10.1002/2013JA019465.

Thampi, S. V., R. T. Tsunoda, L. Jose, and T. K. Pant (2012), Ionogram signatures of large-scale wave structure and their relation to equatorial spread F, *J. Geophys. Res.*, *117*, A08314, doi:10.1029/2012JA017592.

Tiwari, D., A. K. Patra, K. S. Viswanathan, N. Jyoti, C. V. Devasia, K. S. V. Subbarao, and R. Sridharan (2003), Simultaneous radar observations of the electrojet plasma irregularities at 18 and 54.95 MHz over Trivandrum, India, *J. Geophys. Res.*, *108*(A10), 1368, doi:10.1029/2002JA009698.

Tiwari, P., D. Tiwari, G. Surve, and C. Nayak (2012), Sporadic E over Allahabad during the extremely prolonged low solar activity period of 2007–2009, *Indian J. Radio Space Phys.*, *41*(2), 285–293.

Tsunoda, R. T. (2008), Satellite traces: An ionogram signature for large scale wave structure and a precursor for equatorial spread F, *Geophys. Res. Lett.*, *35*, L20110, doi:10.1029/2008GL035706.

Tsunoda, R. T. (2009), Multi-reflected echoes: Another ionogram signature of large-scale wave structure, *Geophys. Res. Lett.*, *36*, L01102, doi:10.1029/2008GL036221.

Viswanathan, K. S., S. P. Namboothiri, and P. B. Rao (1992), VHF and HF radar measurements of E and F region plasma drifts at the magnetic equator, *J. Geophys. Res.*, *97*(A3), 3011–3017, doi:10.1029/91JA02187.

Wright, J. W., and M. L. V. Pitteway (1979), Real-time data acquisition and interpretation capabilities of the Dynasonde: 2. Determination of magnetoionic mode and echolocation using a small spaced receiving array, *Radio Sci.*, *14*, 827–835, doi:10.1029/RS014i005p00827.

Woodman, R. F., J. L. Chau, and R. R. Ilma (2006), Comparison of ionosonde and incoherent scatter drift measurements at the magnetic equator, *Geophys. Res. Lett.*, *33*, L01103, doi:10.1029/2005GL023692.

Yadav, V., B. Kakad, T. K. Pant, A. Bhattacharyya, and D. S. V. V. D. Prasad (2015), Study of equatorial E region irregularities using rare daytime VHF scintillation observations, *J. Geophys. Res. Space Physics*, *120*, 9074–9086, doi:10.1002/2015JA021320.